



Entropy generation for the blood flow in an artery with multiple stenosis having a catheter



A.M. Zidan ^a, L.B. McCash ^b, Salman Akhtar ^c, Anber Saleem ^d, Alibek Issakhov ^e,
 Sohail Nadeem ^{c,*}

^a Department of Mathematics, College of Science King Khalid University, P.O. Box: 9004, Abha 61413, Saudi Arabia

^b School of Mathematics & Actuarial Science, University of Leicester, Leicester LE1 7RH, UK

^c Department of Mathematics, Quaid-i-Azam University 45320, Islamabad 44000, Pakistan

^d Department of Anatomy, School of Dentistry, Shaheed Zulfiqar Ali Bhutto Medical University Islamabad, Pakistan

^e Al-Farabi Kazakh National University, Faculty of Mechanics and Mathematics, av. al-Farabi 71, Almaty, Kazakhstan

Received 11 July 2020; revised 9 April 2021; accepted 24 April 2021

KEYWORDS

Multiple stenosed artery;
 Thrombus;
 Catheter;
 Entropy

Abstract This article explicates the blood flow across an artery with multiple stenosis at outer wall and a thrombus at the centre. The symmetric multiple stenosis and non-symmetric multiple stenosis shapes are both considered in this study. Entropy analysis is also taken into account for a detailed study of irreversibility. The governing equations are interpreted with provided boundary conditions and exact mathematical solutions are developed. Further, these exact solutions are elucidated graphically. Streamlines show that the closed contours are symmetric in shape for symmetric multiple stenosis but non-symmetric in shape for non-symmetric multiple stenosis shape. The increase in multiple stenosis heights, increases the shear stress at wall having multiple stenosis.

© 2021 THE AUTHORS. Published by Elsevier BV on behalf of Faculty of Engineering, Alexandria University. This is an open access article under the CC BY-NC-ND license (<http://creativecommons.org/licenses/by-nc-nd/4.0/>).

1. Introduction

The blood flow is confined across diseased arteries having stenosis. This stenosis evolves by plaque collection due to fats and oils at the walls of such arteries. In certain terrible conditions, this plaque collection can also result in multiple stenosis. In these circumstances, the flow across such arteries is confined at multiple locations due to several stenosis. In his doctoral dissertation, Ponalagusamy [1] first time studied the flow

across such tapered tubes. Mandal [2] considered the power law flow model to illustrate the time dependent flow of blood through such tapered vessels. The distinct shapes of stenosis are also incorporated in Ponalagusamy's [3] study. Vonruden et al. [4] had presented an experimental study for flow of blood across a diseased vessel with multiple stenosis. Misra et al. [5] had theoretically interpreted the blood flow as Casson fluid inside an artery having multiple stenosis. The flow of blood across an artery having multiple stenosis, considering mild case of multiple stenosis along the arterial length was studied by Sreenadh et al. [6]. Nadeem et al. [7] had mathematically explained the flow of carbon nanotube across an artery with multiple stenosis, considering case of variable viscosity.

* Corresponding author.

E-mail address: sohail@qau.edu.pk (S. Nadeem).

Peer review under responsibility of Faculty of Engineering, Alexandria University.

<https://doi.org/10.1016/j.aej.2021.04.058>

1110-0168 © 2021 THE AUTHORS. Published by Elsevier BV on behalf of Faculty of Engineering, Alexandria University. This is an open access article under the CC BY-NC-ND license (<http://creativecommons.org/licenses/by-nc-nd/4.0/>).

Nomenclature

(\bar{r}, \bar{z}) Cylindrical Coordinate
 (u, w) Radial, Axial velocity
 cR Catheter radius
 R Non-stenotic radius of outer tube
 s_l Stenosis length ($l = 1, 2, 3$)
 $n \geq 2$ Multiple stenosis shape parameter
 σ Maximum height of clot
 B_r Brickmann number

θ_0 Non-dimensional ratio of absolute to usual temperature difference
 δ_l^* Stenosis maximum height ($l = 1, 2, 3$)
 d_l Stenosis location ($l = 1, 2, 3$)
 N_S Dimensionless Entropy
 B_e Bejan number
 z_d Axial displacement of clot

Latterly, many researchers have concentrated on the study of blood flow across arteries with a blood clot at their centre position. These blood clots (Thrombus) are more frequently developed in diseased arteries already having tapered walls. Thus, an artery with multiple stenosis gets more chances to have a thrombus as well. This is the worst scenario that almost blocks the blood flow and has deadly consequences. In this situation, the flow is again improved with catheter application. This slender, vacant tube can be placed in such troubled arteries to refine the flow. The flow problem considering both models, (i.e. thrombus and stenosis) was experimentally as well as theoretically studied by Doffin et al. [8]. The macroscopic double-phase flow model for blood flow across a tapered tube by utilizing catheter was mathematically interpreted by Srivastava et al. [9]. Nadeem et al. [10] had mathematically studied the blood flow across a catheterized artery with a mild stenosis. The surgical method used for the placement of moving catheter across a stenosed artery was explained by Mekheimer et al. [11]. The couple stress model of fluid for the mathematical interpretation of blood flow across a diseased tapered artery by making use of a catheter was presented by Reddy [12].

The transfer of heat procedure for blood flow across a tapered artery, considered two phase model, with catheter application was studied by Garcia [13]. Tashtoush et al. [14] had interpreted the heat transfer mechanism of blood flow across a diseased artery with multiple stenosis. The study of temperature for blood flow across diseased tapered arteries, considering various fluid models are presented in the studies [15–18]. Mekheimer et al. [19] had mathematically interpreted the irreversibility of blood flow across a stenosed tube with catheter application by considering entropy generation study case. Some recent bio-mathematical models are also referred as [20–23].

The previously obtained literature work is thoroughly studied, and it is disclosed that the blood flow across a diseased artery having multiple stenosis at outer wall and a thrombus at the centre is not yet explored with application of a catheter. This work explains the blood flow across an artery with multiple stenosis at outer wall and a blood clot at the centre. This confined flow across the diseased artery is refined by using a catheter. The symmetric and non-symmetric multiple stenosis shapes are also considered in this study. This blood flow study includes a Newtonian viscous model. The viscous effects are also incorporated in energy equation by considering viscous dissipation. Entropy analysis is also considered for a detailed study of irreversibility. The governing flow problem equations are interpreted with provided boundary conditions and exact mathematical solutions are developed. Further, these exact

solutions are elucidated graphically. Streamlines show that the closed contours are symmetric in shape for symmetric multiple stenosis but non-symmetric in shape for non-symmetric multiple stenosis shape.

2. Mathematical model

The blood flow across an artery with multiple stenosis at outer wall and a thrombus at the centre is examined. This confined flow across the diseased artery is refined by using a catheter. The symmetric multiple stenosis and non-symmetric multiple stenosis shapes are both considered in this study (see Fig. 1).

The geometries of exterior boundary $\bar{\eta}(z)$, i.e. (wall having multiple stenosis) and inner boundary $\bar{\epsilon}(z)$, i.e. (wall having a thrombus at the centre) are provided in dimensional form [24,25].

$$\bar{\eta}(z) = \begin{cases} R \left[1 - K \left\{ s_l^{n-1} (\bar{z} - d_l) - (\bar{z} - d_l)^n \right\} \right], & d_l \leq \bar{z} \leq d_l + s_l \\ R & \end{cases} \quad (1)$$

$$\bar{\epsilon}(z) = \begin{cases} R [c + f_1(\bar{z})], & d_2 \leq \bar{z} \leq d_2 + s_2 \\ cR & \text{otherwise} \end{cases} \quad (2)$$

The clot's shape depends on choice of $f_1(\bar{z})$. Further, K is defined as

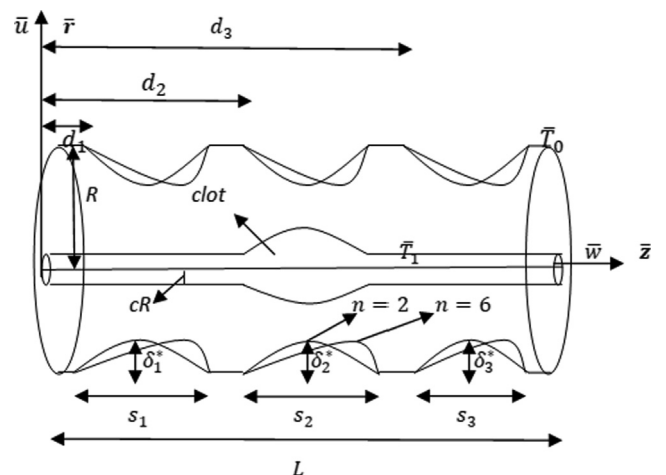


Fig. 1 Geometry of flow Problem.

$$K = \frac{\delta_l^* n^{n/n-1}}{R s_l^n n - 1}. \quad (3)$$

Here the utmost height attained by stenosis is given by δ_l^* at location $z = d_l + \frac{y_l}{n^{1/n-1}}$. The position of each stenosis is measured by d_l and $l = 1, 2, 3$. The stenosis shape is dependent on the value of n and it has symmetric shape for $n = 2$ but for $n = 6$, it has non-symmetric shape. The governing mathematical equations are provided below in their dimensional form [26].

$$\frac{1}{r} \frac{\partial(\bar{r} \bar{u})}{\partial \bar{r}} + \frac{\partial \bar{w}}{\partial \bar{z}} = 0, \quad (4)$$

$$\rho \left[\bar{u} \frac{\partial \bar{u}}{\partial \bar{r}} + \bar{w} \frac{\partial \bar{u}}{\partial \bar{z}} \right] = -\frac{\partial \bar{p}}{\partial \bar{r}} + \mu \left[\frac{\partial^2 \bar{u}}{\partial \bar{r}^2} + \frac{1}{r} \frac{\partial \bar{u}}{\partial \bar{r}} + \frac{\partial^2 \bar{u}}{\partial \bar{z}^2} - \frac{\bar{u}}{r^2} \right]. \quad (5)$$

$$\rho \left[\bar{u} \frac{\partial \bar{w}}{\partial \bar{r}} + \bar{w} \frac{\partial \bar{w}}{\partial \bar{z}} \right] = -\frac{\partial \bar{p}}{\partial \bar{z}} + \mu \left[\frac{\partial^2 \bar{w}}{\partial \bar{r}^2} + \frac{1}{r} \frac{\partial \bar{w}}{\partial \bar{r}} + \frac{\partial^2 \bar{w}}{\partial \bar{z}^2} \right]. \quad (6)$$

$$\rho C_p \left[\bar{u} \frac{\partial \bar{T}}{\partial \bar{r}} + \bar{w} \frac{\partial \bar{T}}{\partial \bar{z}} \right] = k \left[\frac{\partial^2 \bar{T}}{\partial \bar{r}^2} + \frac{1}{r} \frac{\partial \bar{T}}{\partial \bar{r}} + \frac{\partial^2 \bar{T}}{\partial \bar{z}^2} \right] + \mu \left[2 \left\{ \left(\frac{\partial \bar{u}}{\partial \bar{r}} \right)^2 + \left(\frac{\bar{u}}{r} \right)^2 + \left(\frac{\partial \bar{w}}{\partial \bar{z}} \right)^2 \right\} + \left(\frac{\partial \bar{w}}{\partial \bar{r}} + \frac{\partial \bar{u}}{\partial \bar{z}} \right)^2 \right]. \quad (7)$$

The non-dimensional variables are

$$r = \frac{\bar{r}}{R}, z = \frac{\bar{z}}{s_l}, w = \frac{\bar{w}}{u_0}, u = \frac{L \bar{u}}{u_0 \delta_l^*}, p = \frac{R^2 \bar{p}}{u_0 s_l \mu_f}, \theta = \frac{\bar{T} - \bar{T}_0}{\bar{T}_1 - \bar{T}_0},$$

$$\epsilon(z) = \frac{\bar{\epsilon}(z)}{R}, \eta(z) = \frac{\bar{\eta}(z)}{R}, h_l = \frac{d_l}{s_l}, \delta_l = \frac{\delta_l^*}{R},$$

$$B_r = \frac{\mu_f u_0^2}{k_f (\bar{T}_1 - \bar{T}_0)}, S_{G_0} = \frac{k_f (\bar{T}_1 - \bar{T}_0)^2}{\bar{T}_0^2 R^2}, \theta_0 = \frac{\bar{T}_0}{(\bar{T}_1 - \bar{T}_0)}, \quad (8)$$

The case of a mild stenosis is considered by applying these assumptions

$$\delta_l = \frac{\delta_l^*}{R} \ll 1, \frac{R n^{1/n-1}}{s_l} \gg 1. \quad (9)$$

The non-dimensional variables provided in Eq. (8) are utilized in Eqs. (4)–(7) and then the assumptions given in Eq. (9) are used to obtain these dimensionless governing equations.

$$\frac{\partial p}{\partial r} = 0. \quad (10)$$

$$\frac{\partial p}{\partial z} = \frac{\partial^2 w}{\partial r^2} + \frac{1}{r} \frac{\partial w}{\partial r}. \quad (11)$$

$$\frac{\partial^2 \theta}{\partial r^2} + \frac{1}{r} \frac{\partial \theta}{\partial r} + B_r \left(\frac{\partial w}{\partial r} \right)^2 = 0. \quad (12)$$

The relevant dimensionless boundary conditions are

$$w = 0, \text{ at } r = \epsilon(z), \text{ and } w = 0, \text{ at } r = \eta(z). \quad (13)$$

$$\theta = 1, \text{ at } r = \epsilon(z), \text{ and } \theta = 0, \text{ at } r = \eta(z). \quad (14)$$

The geometry of outer boundary $\eta(z)$, i.e. (wall having multiple stenosis) and inner boundary $\epsilon(z)$, i.e. (wall having blood clot at centre) is provided in non-dimensional form. The thrombus model is expressed by suitably selecting $f_1(\bar{z})$ [25].

$$\eta(z) = \begin{cases} 1 - \delta_l \frac{n^{n/n-1}}{n-1} [(z - h_l) - (z - h_l)^n], & h_l \leq z \leq h_l + 1 \\ 1 & \text{otherwise} \end{cases}. \quad (15)$$

$$\epsilon(z) = \begin{cases} c + \sigma e^{-\pi^2(z - z_d - 0.5)^2}, & h_2 \leq z \leq h_2 + 1 \\ c & \text{otherwise} \end{cases}. \quad (16)$$

3. Exact solution

The velocity profile is evaluated exactly by solving Eq. (11) with conditions mentioned in Eq. (13).

$$w = \frac{\left[\frac{\partial p}{\partial z} \{ (-\epsilon^2 + \eta^2) \text{Log}(r) + (r^2 - \eta^2) \text{Log}(\epsilon) + (-r^2 + \epsilon^2) \text{Log}(\eta) \} \right]}{4(\text{Log}(\epsilon) - \text{Log}(\eta))}. \quad (17)$$

The rate of flow for volume is evaluated as

$$Q = \int_{\epsilon}^{\eta} r w dr. \quad (18)$$

The calculated expression for pressure gradient is

$$\frac{dp}{dz} = \frac{16Q(\text{Log}(\epsilon) - \text{Log}(\eta))}{(\epsilon^2 - \eta^2)[- \epsilon^2 + \eta^2 + (\epsilon^2 + \eta^2)(\text{Log}(\epsilon) - \text{Log}(\eta))]} \quad (19)$$

The result interpreted for wall shear stress is

$$\tau_w = -\frac{\partial w}{\partial r} \Big|_{r=\eta} = \frac{-\frac{\partial p}{\partial z} \left[\frac{-\epsilon^2 + \eta^2}{\eta} + 2\eta(\text{Log}(\epsilon) - \text{Log}(\eta)) \right]}{4(\text{Log}(\epsilon) - \text{Log}(\eta))}. \quad (20)$$

The temperature profile is also evaluated exactly by interpreting Eq. (12) with conditions mentioned in Eq. (14)

$$\theta = \frac{1}{64(\text{Log}(\epsilon) - \text{Log}(\eta))^2} \left[-2B_r \left(\frac{\partial p}{\partial z} \right)^2 (\epsilon^2 - \eta^2)^2 (\text{Log}(r))^2 - B_r \left(\frac{\partial p}{\partial z} \right)^2 (r^2 - \eta^2) \text{Log}(\epsilon) \{ -4(\epsilon^2 - \eta^2) + (r^2 + \eta^2) \text{Log}(\epsilon) \} + \left\{ -4B_r \left(\frac{\partial p}{\partial z} \right)^2 (r^2 - \epsilon^2)(\epsilon^2 - \eta^2) + \left(-64 + B_r \left(\frac{\partial p}{\partial z} \right)^2 (2r^4 - 3\epsilon^4 + 4\epsilon^2 \eta^2 - 3\eta^4) \right) \text{Log}(\epsilon) \right\} \text{Log}(\eta) + \left(64 + B_r \left(\frac{\partial p}{\partial z} \right)^2 (-r^4 + \epsilon^4) \right) (\text{Log}(\eta))^2 + \text{Log}(r) \left\{ -4B_r \left(\frac{\partial p}{\partial z} \right)^2 (\epsilon^2 - \eta^2)^2 + \left(64 + B_r \left(\frac{\partial p}{\partial z} \right)^2 (3\epsilon^4 - 4\epsilon^2 \eta^2 + \eta^4) \right) \text{Log}(\epsilon) + \left(-64 + B_r \left(\frac{\partial p}{\partial z} \right)^2 (\epsilon^4 - 4\epsilon^2 \eta^2 + 3\eta^4) \right) \text{Log}(\eta) \right\} \right]. \quad (21)$$

4. Entropy analysis

The equation for entropy analysis in its dimensional form is provided [27].

$$S_G = \frac{k_f}{T_0} \left[\left(\frac{\partial \bar{T}}{\partial r} \right)^2 + \left(\frac{\partial \bar{T}}{\partial z} \right)^2 \right] + \frac{\mu_f}{T_0} \left[2 \left\{ \left(\frac{\partial \bar{u}}{\partial r} \right)^2 + \left(\frac{\bar{u}}{r} \right)^2 + \left(\frac{\partial \bar{w}}{\partial z} \right)^2 \right\} + \left(\frac{\partial \bar{w}}{\partial r} + \frac{\partial \bar{u}}{\partial z} \right)^2 \right]. \tag{22}$$

Now by application of non-dimensional variables mentioned in Eq. (8) and also with use of given assumptions in Eq. (9). The equation in dimensionless form for entropy analysis is

$$N_S = \frac{S_G}{S_{G_0}} = \left(\frac{\partial \theta}{\partial r} \right)^2 + \theta_0 B_r \left(\frac{\partial w}{\partial r} \right)^2. \tag{23}$$

Eq. (23) is sum of two terms and first term is basically entropy produced by measurable difference of temperature ($N_{S_{cond}}$) while the later term is entropy caused by viscous results ($N_{S_{visc}}$). Moreover, Bejan number appears as

$$Be = \frac{N_{S_{cond}}}{N_{S_{cond}} + N_{S_{visc}}} = \frac{\left(\frac{\partial \theta}{\partial r} \right)^2}{\left(\frac{\partial \theta}{\partial r} \right)^2 + \theta_0 B_r \left(\frac{\partial w}{\partial r} \right)^2}. \tag{24}$$

5. Results and discussion

The exact results evaluated for velocity, pressure gradient, wall shear stress τ_w , temperature and entropy are graphically explained in this section. These graphs elucidate the results for both symmetric multiple stenosis, (i.e. $n = 2$) and non-symmetric multiple stenosis, (i.e. $n = 6$). In Fig. 2a, Fig. 2b, Fig. 2c and Fig. 2d, the velocity $w(r, z)$ for the governing flow problem is plotted against the radial coordinate r , for various enhancing values of dimensionless parameters of interest. Fig. 2a reveals that the velocity, in case of symmetric as well as non-symmetric shapes of stenosis, increases in the middle of channel with enhancing δ_l . It is clear from this graph that velocity increments in the middle, as the channel turns narrow with enhancing δ_l but it reduces towards the multiple stenosis wall. For both symmetric as well as non-symmetric shapes of multiple stenosis, Fig. 2b shows enhance in the velocity for increasing Q . Fig. 2c displays decrease in the velocity at wall

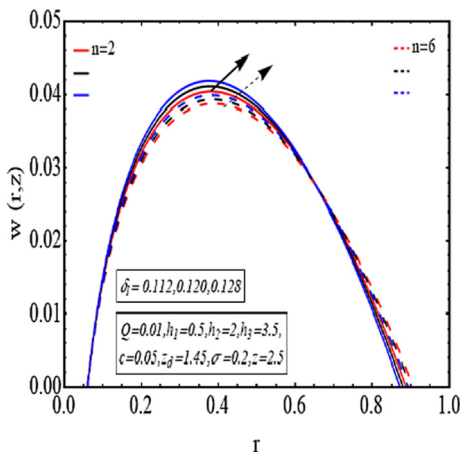


Fig. 2a Velocity for. δ_l .

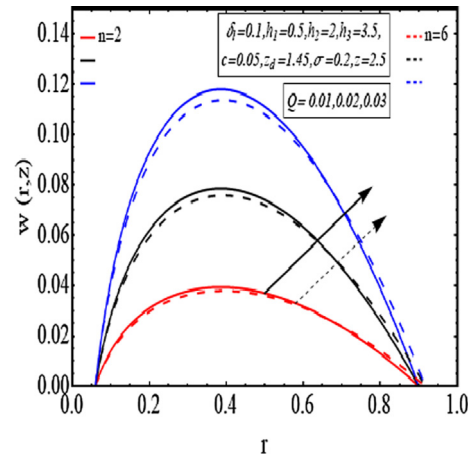


Fig. 2b Velocity for Q .

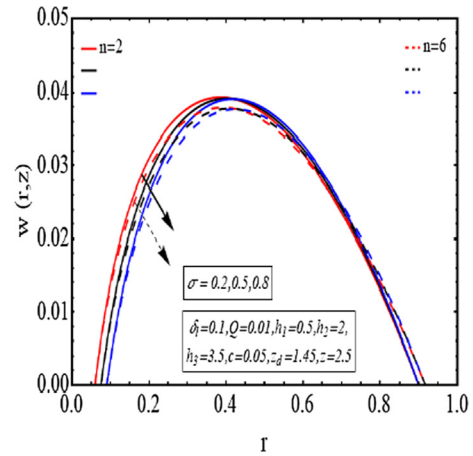


Fig. 2c Velocity for σ .

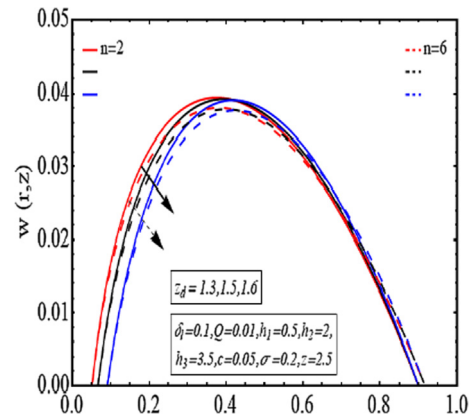


Fig. 2d Velocity for z_d .

with clot whether stenosis has symmetric or non-symmetric shape, but velocity depicts fixed behaviour at multiple stenosis wall for increasing clot height σ . There is decrease in the velocity at the clot wall as the axial displacement z_d of clot increases but the behaviour of velocity profile is not changing near multiple stenosis wall, as shown in Fig. 2d. In all these velocity

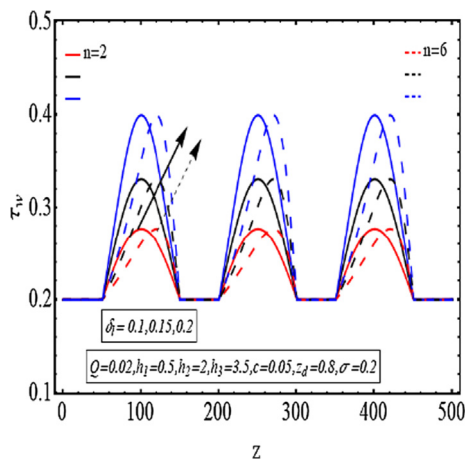


Fig. 3a τ_w for δ_j .

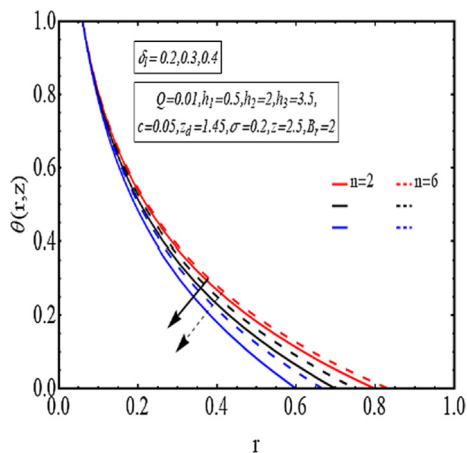


Fig. 4b Temperature for δ_j .

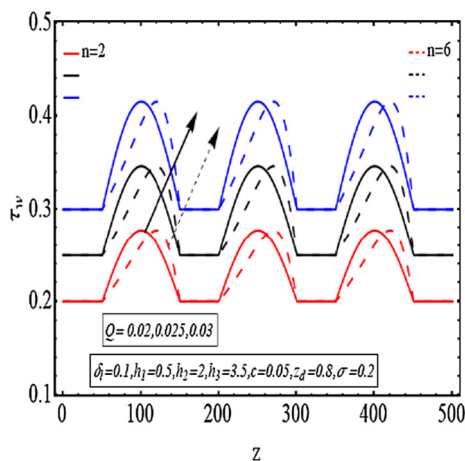


Fig. 3b τ_w for Q .

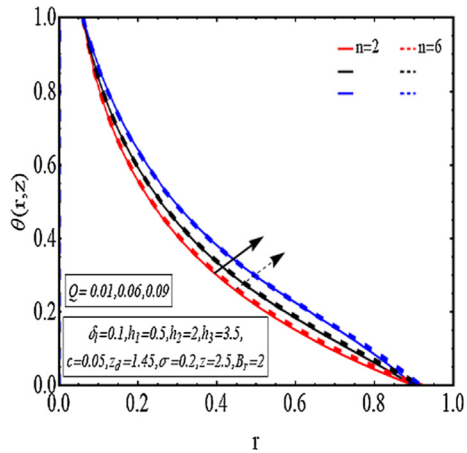


Fig. 4c Temperature for Q .

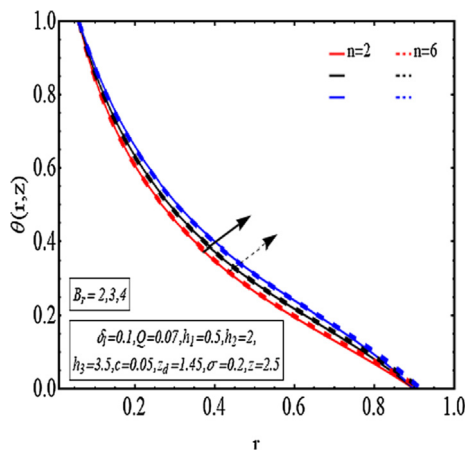


Fig. 4a Temperature for B_r .

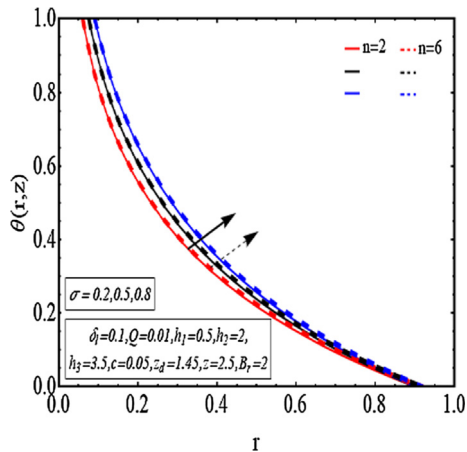


Fig. 4d Temperature for σ .

graphs, it is observed that the velocity for non-symmetric shape of multiple stenosis is lower than the symmetric shape.

In Fig. 3a, Fig. 3b, τ_w the wall shear stress against z -axis is plotted. Fig. 3a reveals that τ_w varies directly with incrementing δ_j . It is seen that the enhance in multiple stenosis heights,

enhances the shear stress at wall having multiple stenosis. Further, τ_w also varies directly with increasing flow rate Q , as displayed in Fig. 3b. In Fig. 4a, Fig. 4b, Fig. 4c and Fig. 4d, the temperature against r -axis is plotted for various parameters of physical interest. For multiple stenosis having symmetric or

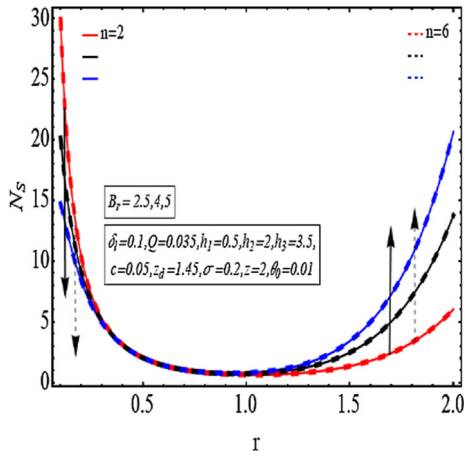


Fig. 5a Entropy for B_r .

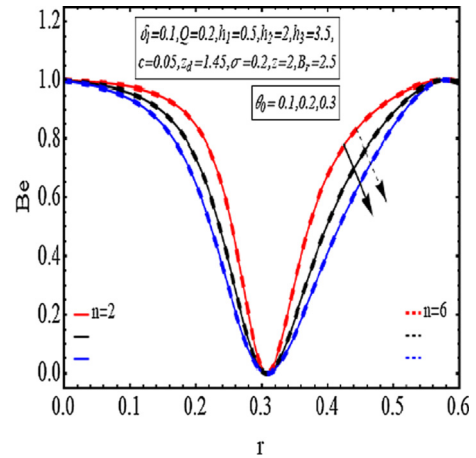


Fig. 6b Bejan number for θ_0 .

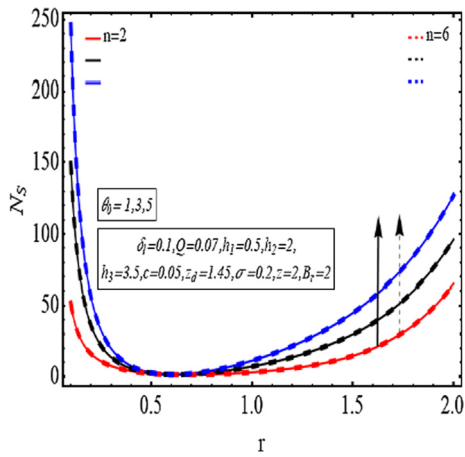


Fig. 5b Entropy for θ_0 .

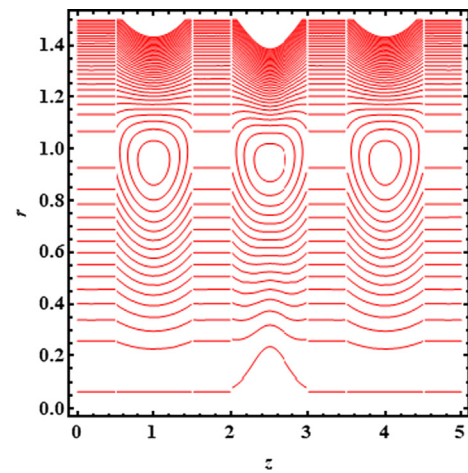


Fig. 7a Streamlines at $Q = 2, n = 2$.

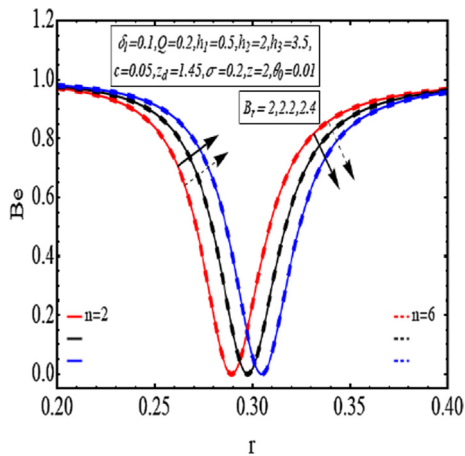


Fig. 6a Bejan number for B_r .

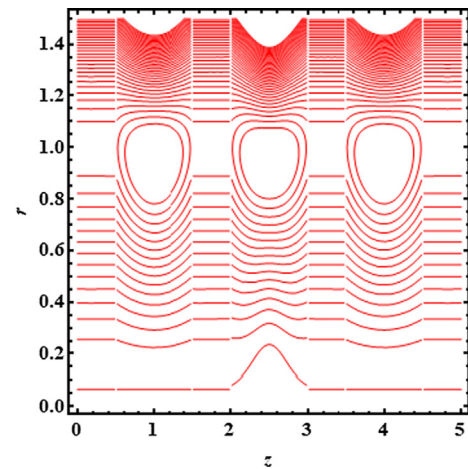


Fig. 7b Streamlines at $Q = 2.2, n = 2$.

non-symmetric shapes, Fig. 4a shows that when the value of B_r increments, there is enhance in temperature. The temperature varies inversely for incrementing δ_i , as depicted in Fig. 4b. The temperature enhances with enhancing Q , shown in Fig. 4c. In Fig. 4d, it is revealed that temperature enhances

for increasing clot height σ . The irreversibility is discussed by plotting graphs for entropy, shown in Fig. 5a, Fig. 5b. Fig. 5a reveals that N_s behaves differently at different walls, i.e. it decreases with wall having thrombus but it enhances at

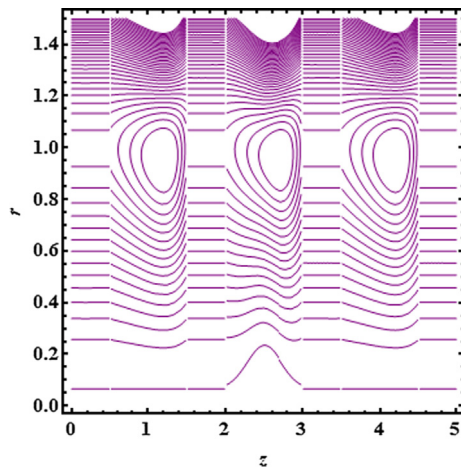


Fig. 7c Streamlines at $Q = 2, n = 6$.

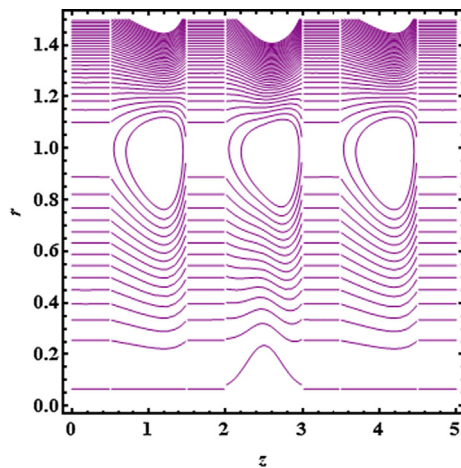


Fig. 7d Streamlines at $Q = 2.2, n = 6$.

the multiple stenosis wall for incrementing B_r . The entropy varies directly with both thrombus and multiple stenosis wall for incrementing θ_0 , as displayed in Fig. 5b. In Fig. 6a, Fig. 6b Bejan number is discussed with help of graphs. B_e has distinct behaviour at distinct walls, i.e. it increases with thrombus wall but drops with multiple stenosis wall for increasing values of B_r , revealed in Fig. 6a. B_e declines everywhere for increasing θ_0 , depicted in Fig. 6b. In Fig. 7a, Fig. 7b, Fig. 7c and Fig. 7d the flow behaviour is seen by plotting streamlines for this problem. Fig. 7a and Fig. 7b are plotted for symmetric shape of multiple stenosis and it is clearly seen that the trapping increments in size but declines in count for increasing Q . Further, the symmetric shapes of multiple stenosis at one wall and the clot at other wall can clearly be seen. Fig. 7c and Fig. 7d are plotted for non-symmetric multiple stenosis shape and here again the trapping increments in size but declines in count for enhancing Q . Also, the non-symmetric shapes of multiple stenosis at one wall and thrombus at other wall are clearly observed. Moreover, the closed contours are symmetric in shape for symmetric multiple stenosis but non-symmetric in shape for non-symmetric multiple stenosis shape.

6. Conclusions

The blood flow across an artery with multiple stenosis at outer wall and a thrombus at the centre is mathematically elucidated. This confined flow across the diseased artery is refined by using a catheter. The symmetric multiple stenosis and non-symmetric multiple stenosis shapes are also considered in this study. The key results are

- The velocity enhances in the middle, as the channel turns narrow with enhancing δ_l but it reduces towards the multiple stenosis wall.
- The velocity for non-symmetric shape of multiple stenosis is lower than the symmetric shape.
- The temperature varies inversely for incrementing δ_l .
- N_S behaves differently at different walls, i.e. it decreases with wall having thrombus but it enhances at the multiple stenosis wall for incrementing B_r .
- The closed contours are symmetric in shape for symmetric multiple stenosis but non-symmetric in shape for non-symmetric multiple stenosis shape.

Declaration of Competing Interest

The authors declare that they have no known competing financial interests or personal relationships that could have appeared to influence the work reported in this paper.

Acknowledgement

The first author (A. M. Zidan) extend his appreciation to the deanship of scientific research at King Khalid University, Abha 61413, Saudi Arabia for funding this work through the grant number G.R.P/ 45/42.

References

- [1] R. Ponalagusamy, Blood flow through Stenosed Tube Doctoral dissertation, Ph. D Thesis, IIT, Bombay, India, 1986.
- [2] P.K. Mandal, An unsteady analysis of non-Newtonian blood flow through tapered arteries with a stenosis, *Int. J. Non-Linear Mech.* 40 (1) (2005) 151–164.
- [3] R. Ponalagusamy, Blood flow through an artery with mild stenosis: a two-layered model, different shapes of stenoses and slip velocity at the wall, *J. Appl. Sci.* 7 (7) (2007) 1071–1077.
- [4] W.J. Vonruden, F.W. Blaisdell, A.D. Hall, A.N. Thomas, Multiple Arterial Stenoses: Effect on Blood Flow: An Experimental Study, *Arch. Surg.* 89 (2) (1964) 307–315.
- [5] J.C. Misra, A. Sinha, G.C. Shit, Theoretical analysis of blood flow through an arterial segment having multiple stenoses, *J. Mech. Med. Biol.* 8 (02) (2008) 265–279.
- [6] S. Sreenadh, A.R. Pallavi, B.H. Satyanarayana, Flow of a Casson fluid through an inclined tube of non-uniform cross section with multiple stenoses, *Adv. Appl. Sci. Res.* 2 (5) (2011) 340–349.
- [7] S. Nadeem, S. Ijaz, Single wall carbon nanotube (SWCNT) examination on blood flow through a multiple stenosed artery with variable nanofluid viscosity, *AIP Adv.* 5 (10) (2015).
- [8] J. Doffin, F. Chagneau, Oscillating flow between a clot model and a stenosis, *J. Biomech.* 14 (3) (1981) 143–148.
- [9] V.P. Srivastava, R. Rastogi, Blood flow through a stenosed catheterized artery: effects of hematocrit and stenosis shape, *Comput. Math. Appl.* 59 (4) (2010) 1377–1385.

- [10] S. Nadeem, S. Ijaz, Nanoparticles analysis on the blood flow through a tapered catheterized elastic artery with overlapping stenosis, *Eur. Phys. J. Plus* 129 (11) (2014) 249.
- [11] K.S. Mekheimer, M.A. El Kot, Mathematical modeling of axial flow between two eccentric cylinders: application on the injection of eccentric catheter through stenotic arteries, *Int. J. Non-Linear Mech.* 47 (8) (2012) 927–937.
- [12] J.R. Reddy, D. Srikanth, S.K. Murthy, Mathematical modelling of pulsatile flow of blood through catheterized unsymmetric stenosed artery—Effects of tapering angle and slip velocity, *Eur. J. Mech.-B/Fluids* 48 (2014) 236–244.
- [13] A.E. Garcia, D.N. Riahi, Two-phase blood flow and heat transfer in an inclined stenosed artery with or without a catheter, *Int. J. Fluid Mech. Res.* 41 (1) (2014) 16–30.
- [14] B. Tashtoush, A. Magableh, Magnetic field effect on heat transfer and fluid flow characteristics of blood flow in multi-stenosis arteries, *Heat Mass Transf.* 44 (3) (2007) 297–304.
- [15] N.S. Akbar, S. Nadeem, Simulation of heat and chemical reactions on Reiner Rivlin fluid model for blood flow through a tapered artery with a stenosis, *Heat Mass Transf.* 46 (5) (2010) 531–539.
- [16] N.S. Akbar, S. Nadeem, C. Lee, Influence of heat transfer and chemical reactions on Williamson fluid model for blood flow through a tapered artery with a stenosis, *Asian J. Chem.* 24 (6) (2012) 2433–2441.
- [17] S. Nadeem, N.S. Akbar, T. Hayat, A.A. Hendi, Influence of heat and mass transfer on Newtonian biomagnetic fluid of blood flow through a tapered porous arteries with a stenosis, *Transp. Porous Media* 91 (1) (2012) 81–100.
- [18] S. Nadeem, N.S. Akbar, Influence of heat and chemical reactions on Walter's B fluid model for blood flow through a tapered artery, *J. Taiwan Inst. Chem. Eng.* 42 (1) (2011) 67–75.
- [19] K.S. Mekheimer, A.Z. Zaher, A.I. Abdellateef, Entropy hemodynamics particle-fluid suspension model through eccentric catheterization for time-variant stenotic arterial wall: Catheter injection, *IJGMM* 16 (11) (2019) 1950164–1950496.
- [20] M. Sher, K. Shah, Z.A. Khan, H. Khan, A. Khan, Computational and theoretical modeling of the transmission dynamics of novel COVID-19 under Mittag-Leffler power law, *Alexandria Eng. J.* 59 (5) (2020) 3133–3147.
- [21] A. Khan, J.F. Gómez-Aguilar, T. Abdeljawad, H. Khan, Stability and numerical simulation of a fractional order plant-nectar-pollinator model, *Alexandria Eng. J.* 59 (1) (2020) 49–59.
- [22] A. Khan, T. Abdeljawad, J.F. Gómez-Aguilar, H. Khan, Dynamical study of fractional order mutualism parasitism food web module, *Chaos, Solitons Fractals* 134 (2020) 109685, <https://doi.org/10.1016/j.chaos.2020.109685>.
- [23] J.F. Gomez-Aguilar, T. Cordova-Fraga, T. Abdeljawad, A. Khan, H. Khan, Analysis of fractal-fractional malaria transmission model, *Fractals* (2020) 2040041.
- [24] K.S. Mekheimer, M.H. Haroun, M.A. Elkot, Effects of magnetic field, porosity, and wall properties for anisotropically elastic multi-stenosis arteries on blood flow characteristics, *Appl. Math. Mech.* 32 (8) (2011) 1047–1064.
- [25] G. Jayaraman, A. Sarkar, Nonlinear analysis of arterial blood flow—steady streaming effect, *Nonlinear Anal. Theory Methods Appl.* 63 (5-7) (2005) 880–890.
- [26] N.S. Akbar, Entropy generation and energy conversion rate for the peristaltic flow in a tube with magnetic field, *Energy* 82 (2015) 23–30.
- [27] A. Bejan, A study of entropy generation in fundamental convective heat transfer, 1979.